International Journal of Infrared and Millimeter Waves, Vol. 14, No. 12, 1993

MICROWAVE CAVITY PERTURBATION TECHNIQUE: PART I: PRINCIPLES

Olivier Klein,* Steve Donovan,† Martin Dressel, and George Grüner
Department of Physics and Solid State Science Center
University of California, Los Angeles
Los Angeles, California 90024-1547

Received September 22, 1993

Abstract

This report reviews the analysis used to extract the complex conductivity of a compound from a microwave cavity perturbation measurement. We intend to present a generalized treatment valid for any spheroidally shaped sample of arbitrary conductivity which is placed at either the electric or magnetic field antinode of the cavity. To begin with, we establish the relationship between the measured parameters and the conductivity for a spherical sample. Next, we extend these results to the case of spheroids; and for the first time, we cover all different configurations that one can possibly use to study an arbitrary conducting sample inside a cavity: in particular, all possible orientations of the sample with respect to the applied field are solved.

Keywords: electrodynamic response, surface impedance, microwave cavity perturbation theory

1 Introduction

Among the different techniques available to determine the conductivity in the micro and millimeter wave spectral range (e.g. a bridge or quasi-optical

*present address: Physics Department, Massachusetts Institute of Technology, 77 Massachusetts Ave., Cambridge MA 02139

†present address: Max-Planck-Institut für Festkörperforschung, Heisenbergstr. 1, D 70569 Stuttgart, Germany

0195-9271/93/1200-2423$07.00/0

device), the cavity perturbation technique is one of the most widely used [1, 2] because of its relative simplicity. In this technique one measures the adiabatic change of the characteristics of a resonator upon the introduction of a foreign body (the sample under investigation). The foreign body must be small compared to the spatial variation of the field (quasi-static limit [3]) and its disturbing influence must not be strong enough to force a jump from the unperturbed cavity mode. The perturbation is viewed as a serial expansion in powers of the filling factor (the volume of the sample V_s divided by the volume of the cavity V_c) and only first order effects are accounted for in this analysis. Although the maximum sample size is bounded with this technique, the measurement sensitivity is greatly enhanced by the confinement of the electromagnetic energy in a resonating structure with a high quality factor Q (typically on the order of 10^4).

In this paper we intend to review the different theoretical aspects which are needed in order to extract the intrinsic material properties of a sample. Several authors have previously studied this problem in a variety of limiting cases: Champlin and Krongard [4] together with Brodwin and Parsons [5] solved the problem exactly for a sphere placed in the maximum of either the magnetic or electric field; Buranov and Shchegolev [6] examined the case of a prolate spheroid in the electric field maximum under the condition that the electromagnetic radiation penetrated uniformly within the sample (depolarization regime); Cohen [7] together with work by Ong [8] investigated a prolate spheroid in the electric field maximum in which the electromagnetic radiation was confined to a small volume near the surface of the sample (skin depth regime). To our knowledge, no general study has been made for a uniaxial spheroid in the maximum of the magnetic field, or for an oblate spheroid in the electric field maximum. Expanding on these previous solutions, we will present the solutions in both limits for the case of a uniaxial spheroid. In addition, we will present an approximation scheme whereby one may determine the solutions for an arbitrary value of the conductivity.

This paper is one of a series of three which is intended to provide a comprehensive review of both the different theoretical and experimental techniques which are commonly used in this field. In Part II [9], we will review the modern technical developments and describe the experimental scheme which is used by our group. Finally, in Part III [10], we will present the results obtained using these techniques with an emphasis on the broad range of applicability.

2 Definitions

2.1 Material Properties

We study the response of a compound to an external electromagnetic excitation of the form $\exp(i\mathbf{q}\cdot\mathbf{r} - i\omega t)$. This response is defined as the ratio of any couple of conjugate variables [11] and it is an intrinsic parameter (i.e. independent of the field strength) if we only retain first order terms (nonlinear effects are neglected). It is then a 3-dimensional tensor of complex eigenvalues whose real and imaginary parts are related through the Kramers-Kronig relations [12] and are generally dependent on both $\mathbf{q}$ and ω. In a microwave experiment, the integrated $\mathbf{q}$ dependence of the response is probed, because the photons have a large wavelength. The characteristic length scale of the response is then fixed by some other parameters, such as the mean free path, the coherence length or the sample size (in the case of thin films).

The complex conductivity $\hat{\sigma}(\mathbf{q},\omega) = \sigma_1 + i\sigma_2$ is defined as the ratio of the current density over the incident electric field

$$\frac{\mathbf{J}(\mathbf{q},\omega)}{\mathbf{E}(\mathbf{q},\omega)} \equiv \hat{\sigma}(\mathbf{q},\omega). \tag{1}$$

As there are many equivalent representations of the electromagnetic response of a system, and since several different conventions are widely used in the literature, we will review them briefly.

The complex permittivity is defined by

$$\hat{\epsilon} = \epsilon_1 + i\epsilon_2 = \epsilon_\infty + 4\pi i\frac{\hat{\sigma}}{\omega}, \tag{2}$$

where ϵ_∞ is the dielectric constant due to the high frequency response. The complex refractive index $\hat{n}_o = \sqrt{\hat{\epsilon}}$ and the complex wavevector inside the medium is given by

$$\hat{k} = \frac{\omega}{c_o}\sqrt{\hat{\mu}\hat{\epsilon}}, \tag{3}$$

where c_o is the speed of light in vacuum. The skin depth $\delta = 1/\mathrm{Im}(\hat{k})$ is the characteristic length scale over which an external electromagnetic wave is damped inside a material. If δ is small compared with the minimum sample dimension, the field is screened from the interior of the sample; this is the so-called skin depth regime. The electric susceptibility is related to the permittivity through the relation

$$\hat{\chi}_e \equiv \frac{\hat{\epsilon} - 1}{4\pi}. \tag{4}$$

In the case of magnetic materials, a complex permeability $\hat{\mu}$ is used which can also depend on the conductivity of the material (this is true even for a non-magnetic material, where $\mu_{dc} = 1$; see below). The magnetic susceptibility is defined as

$$\hat{\chi}_m \equiv \frac{\hat{\mu} - 1}{4\pi}. \tag{5}$$

2.2 Geometrical Effects

For clarity, it is important to separate intrinsic effects (e.g. those due to the material properties) from extrinsic ones (e.g. geometrical effects). A sample in an externally applied field (the field far from the sample surface, denoted by calligraphic letters) sees a local field (or field in the sample, written in roman letters) that can always be expressed as the sum of the applied field plus a correction field (called the depolarization field) proportional to the former. This result is a direct consequence of the linearity of Maxwell's equations. The depolarization field is composed of two factors; one originates from the sample susceptibility $\hat{\chi}$ (intrinsic) and the other is due to the magnification of the local field caused by geometrical effects (extrinsic). The geometrical effects are generally expressed in terms of a 3×3 matrix n (a tensor of rank 1) which is defined by the following equation

$$\mathbf{E} = \mathcal{E} - 4\pi n \cdot \mathbf{P} \quad \text{in the electric field,} \tag{6}$$

$$\mathbf{H} = \mathcal{H} - 4\pi n \cdot \mathbf{M} \quad \text{in the magnetic field,} \tag{7}$$

where $\mathbf{P}$ and $\mathbf{M}$ are the polarization and magnetization of the sample respectively, defined by

$$\mathbf{P} = \hat{\chi}_e \mathbf{E}, \tag{8}$$

$$\mathbf{M} = \hat{\chi}_m \mathbf{H}. \tag{9}$$

This definition of the susceptibility must not be confused with the polarizability $\hat{\alpha}$ which includes the geometrical shape of the body, and is defined by

$$\mathbf{P} = \hat{\alpha}_e \mathcal{E}, \tag{10}$$

$$\mathbf{M} = \hat{\alpha}_m \mathcal{H}. \tag{11}$$

In general both the susceptibility and polarizability are tensors whose principal axes do not necessarily correspond to the principal axes of the ellipsoid. For the sake of simplicity, we will hereafter assume that the principal axes of

the response functions coincide with the principal axes of the ellipsoid and therefore all three tensors may be simultaneously diagonalized.

Additionally, the depolarization field is generally non-uniform within the sample [13]. However, ellipsoidally shaped samples present a special case and a uniform external field produces a uniform depolarization field inside the specimen [12]. The depolarization matrix n of an ellipsoid is diagonal in its principal basis and these elements have been calculated by Osborn [14]. The results of this calculation are displayed in the Appendix A along with expressions in several limiting cases.

The value of the polarization and/or magnetization of the sample can depend strongly on the orientation of the sample with respect to the external field. In an oversimplified view, a small depolarization factor $n \ll 1$ increases as the radii of curvature of the surface (e.g. a needle edge will have a small n, while a flat surface will have an n which approaches unity). Restraining our study to cases where the local field is null (i.e. $\mathbf{E} = \mathbf{H} = 0$, e.g. as is found far inside a good conductor), the sample orientation with a maximum polarization is generally different than the orientation of maximum magnetization.

In the electric field, one finds from Eq. (6)

$$\mathbf{P} = \frac{\mathcal{E}}{4\pi n}. \tag{12}$$

The maximum polarization occurs in the orientation with the minimum depolarization factor (this is the so-called edge-effect). For a needle-shaped sample (prolate spheroid), this corresponds to the case where the external field points along the needle axis. However, in the magnetic field one finds from Eq. (7)

$$\mathbf{M} = \frac{\mathcal{H}}{4\pi(n-1)}. \tag{13}$$

The maximum magnetization thus occurs when the depolarization factor is maximized (the maximum value of n is 1). For a flat disk-shaped sample (oblate spheroid) this corresponds to the case where the external field is normal to the plane of the disk.

2.3 Surface Impedance

In the study of highly conducting specimens at microwave frequencies, the parameter usually measured is the surface impedance, a complex number,

$\hat{Z}_s = R_s - iX_s$, where R_s is the surface resistance and X_s is the surface reactance. The surface impedance is defined [3] as the ratio of the electric and magnetic field at the surface of the metal $\hat{Z}_s \equiv \mathbf{E}_{||}/\mathbf{H}_{||}$ where the $||$ sign indicates the field component in the plane of the surface. This definition is unitless, independent of the surface geometry and normalized by the impedance of the vacuum $Z_o = 4\pi/c_o = 377\ \Omega$.

At high frequency $f = \omega/2\pi$, the field penetrates into the sample on a length scale, $1/\mathrm{Im}(\hat{k})$, where $\hat{k}$ is the wavevector inside the material; this length is either the skin depth in the normal state or the penetration depth in the superconducting phase. It is assumed that the sample surface is flat at the scale of $1/\mathrm{Im}(\hat{k})$.

For most metals the relation between the current and the field is a *local* one, i.e. the current density at one point in the conductor depends only on the field at that position (Ohm's law). This condition presupposes that the electron mean-free-path (ℓ) is small compared with the distances over which the field varies (the skin-depth δ). In this case the field decays exponentially as it penetrates in the sample and the surface impedance is given by

$$\hat{Z}_s = \sqrt{\frac{\hat{\mu}}{\hat{\epsilon}}} = \sqrt{\hat{\mu}\omega/4\pi i\hat{\sigma}}. \tag{14}$$

For a good metal $\sigma_1 \gg \sigma_2$ in the millimeter wave frequency range, and $1/\mathrm{Im}(\hat{k})$ is called the classical skin-depth

$$\delta = \frac{c_o}{\sqrt{2\pi\omega\sigma_1}}. \tag{15}$$

In this regime the surface resistance and reactance have the simple form

$$R_s = X_s = \frac{\omega}{c_o}\frac{\delta}{2}, \tag{16}$$

where it was assumed that the frequency is low enough that electromagnetic oscillations within the mean free path can be neglected. The simplest theory that describes scattering effects is the Drude model

$$\hat{\sigma} = \frac{n_e e^2 \tau}{m}\frac{1}{1 - i\omega\tau}, \tag{17}$$

where n_e is the electron density and m the electron mass. The regime studied above corresponds to the case where $\omega\tau \ll 1$ (Hagen-Rubens limit). The other limit is when $\omega\tau \gg 1$ (the relaxation limit). The correction factors at the cross-over are listed in Table 1.

Table 1: *Correction factor for the electrodynamic properties of a Drude metal in the local regime. We abbreviate* $x = \omega\tau$, $\sigma_o = \sigma(\omega = 0)$, *and* $\delta_o = c_o/(2\pi\omega\sigma_o)^{1/2}$.

	Hagen-Rubens regime $x < 1$	Relaxation regime $x > 1$
$R_s = \frac{\omega}{c_o}\frac{\delta_o}{2}\times$	$(1 - \frac{x}{2} + \frac{x^2}{8} + \mathcal{O}[x^3])$	$(\frac{1}{\sqrt{2x}} - \frac{1}{2(2x)^{5/2}} + \mathcal{O}[x^{-9/2}])$
$X_s = \frac{\omega}{c_o}\frac{\delta_o}{2}\times$	$(1 + \frac{x}{2} + \frac{x^2}{8} + \mathcal{O}[x^3])$	$(\sqrt{2x} + \frac{1}{2(2x)^{3/2}} + \mathcal{O}[x^{-7/2}])$
$\frac{X_s}{R_s} =$	$(1 + x + \frac{x^2}{2} + \mathcal{O}[x^3])$	$(2x + \frac{1}{2x} - \frac{1}{8x^3} + \mathcal{O}[x^{-5}])$
$\delta = \delta_o\times$	$(1 - \frac{x}{2} + \frac{5x^2}{8} + \mathcal{O}[x^3])$	$(\sqrt{\frac{x}{2}} + \frac{3}{2(2x)^{3/2}} + \mathcal{O}[x^{-7/2}])$

The opposite limit occurs when $\delta \ll \ell$ and the classical theory is no longer valid [15] (the wave propagation is not exponential). This limit is called the *anomalous regime* and all the equations derived above have to be modified. The exact solution is elaborate [16] but the correct result can be obtained (within a numerical prefactor) with the following over-simplified picture. Suppose that only a fraction $\eta\delta/\ell$ of the electrons can contribute to the conductivity. If we solve Eq. (15) self-consistently, the skin depth expression becomes

$$\delta^3 = \frac{c^2\ell}{2\pi\eta\sigma_1\omega}. \tag{18}$$

The factor η was computed by Reuter and Sondheimer [16] for both specular scattering ($\eta = 3^{11/2}\pi/128 \sim 10$) and diffuse scattering ($\eta = 4\pi/\sqrt{3} \sim 7$). In either case, the expression for the surface resistance is

$$R_s = \frac{X_s}{\sqrt{3}} = \frac{2\pi\omega}{c^2}\left(\frac{c^2\ell}{2\pi\eta\sigma_1\omega}\right)^{1/3}. \tag{19}$$

3 Cavity Perturbation

A variety of resonant devices are available in the microwave and millimeter wave spectral range (e.g. microwave cavity, split ring resonator, Fabry-Perot resonator). The theoretical techniques we will discuss were originally developed for microwave cavities, however we would like to stress that all of the results to be discussed here are equally applicable to any resonant device.

3.1 Cavity Characteristics

Above a lower cut-off frequency, a resonant cavity can sustain many standing wave modes and near each resonant frequency, the power absorption spectrum has a Lorentzian shape [12]

$$A(\omega) = \frac{1}{4(\omega - \omega_o)^2 + (2\pi\Gamma)^2}, \tag{20}$$

where $f_o = \omega_o/2\pi$ is the center frequency and Γ is the bandwidth or full frequency width at half-maximum. f_o and Γ are the two characteristics of the resonator and their ratio gives the quality factor Q of the cavity, defined as

$$Q \equiv \frac{f_o}{\Gamma} = \frac{\omega_o <W>}{L}, \tag{21}$$

where $<W>$ is the time-averaged energy stored in the cavity and L the energy loss per cycle. The simplest formulation of this problem can be made with the use of a complex frequency notation

$$\hat{\omega} \equiv \omega_o - i\frac{\omega_o}{2Q}. \tag{22}$$

3.2 The Polarizability

The principle of the cavity perturbation technique is to measure separately the cavity characteristics both before (o) and after (s) a small sample has been inserted. The change in the complex frequency is

$$\Delta\hat{\omega} = \hat{\omega}_s - \hat{\omega}_o. \tag{23}$$

If the change $\Delta\hat{\omega}$ is adiabatic, then the product of the period and the time averaged energy stored is invariant [17] (Boltzmann-Ehrenfest theorem)

$$\frac{<W>}{\hat{\omega}} = \text{constant}. \tag{24}$$

This implies that

$$\frac{\Delta \langle W \rangle}{\langle W \rangle} = \frac{\Delta\hat{\omega}}{\hat{\omega}} \sim \frac{f_s - f_o}{f_o} - \frac{i}{2}\left(\frac{1}{Q_s} - \frac{1}{Q_o}\right), \tag{25}$$

$$\langle W \rangle = \frac{1}{16\pi}\int_{V_c} (|\mathcal{E}(\mathbf{r})|^2 + |\mathcal{H}(\mathbf{r})|^2) dv, \tag{26}$$

$$\Delta \langle W \rangle = -\frac{1}{4}\int_{V_s} (\mathbf{P}\cdot\mathcal{E}^* + \mathbf{M}\cdot\mathcal{H}^*) dv. \tag{27}$$

In our definition, Δ is the variation caused by the introduction of a foreign body into the resonating structure, $\Delta f = f_s - f_o$ is the frequency shift and $\Delta\Gamma = 1/Q_s - 1/Q_o$ the change in the width of the resonance.

For ellipsoidal samples, the spatial dependence of the depolarization field can be omitted (see above) and the quantity should be evaluated at the center of the sample (e.g. $\mathbf{P} = \mathbf{P}(\mathbf{r}_0)$ if the sample is located at the position $\mathbf{r} = \mathbf{r}_0$). If we put the sample in the antinode of the electric field ($\mathcal{H} = 0$), then

$$\mathbf{P} = \hat{\alpha}_e \mathcal{E}, \tag{28}$$

$$\frac{\Delta\hat{\omega}}{\omega} = -\frac{\hat{\alpha}_e}{4} V_s \frac{|\mathcal{E}|^2}{\langle W \rangle} = -4\pi\gamma\hat{\alpha}_e. \tag{29}$$

where $\gamma = \gamma_o V_s / V_c$ and γ_o is a constant that depends only on the resonance mode of the cavity

$$\gamma_o = \frac{|\mathcal{E}|^2}{16\pi\langle W \rangle} V_c = \frac{|\mathcal{E}|^2}{2\langle |\mathcal{E}|^2 \rangle}, \tag{30}$$

$$\langle |\mathcal{E}|^2 \rangle = \frac{1}{V_c}\int_{V_c} |\mathcal{E}(\mathbf{r})|^2 dv. \tag{31}$$

The values of the constant γ_o are given in Appendix B for the TE_{011} mode of a cylindrical cavity. If the sample is in the antinode of the magnetic field, Eqs. (28)-(31) will be equivalent but with $\mathcal{E}$ replaced by $\mathcal{H}$ and $\mathbf{P}$ by $\mathbf{M}$.

In conclusion, the absorption of electromagnetic waves by small particles is proportional to the polarizability of the sample

$$\frac{\Delta\hat{\omega}}{\omega} = -4\pi\gamma\hat{\alpha}. \tag{32}$$

3.3 Helmholtz Equation

As we have just seen in the previous section, the problem of determining $\Delta\hat{\omega}/\omega$ has been reduced to finding the polarizability of an arbitrarily shaped

sample. This requires one to solve the Helmholtz differential equation [12]

$$\nabla^2 \mathbf{E}(\mathbf{r}) = 0 \qquad \mathbf{r} \text{ outside the sample} \tag{33}$$

$$\nabla^2 \mathbf{E}(\mathbf{r}) + \hat{k}^2 \mathbf{E}(\mathbf{r}) = 0 \qquad \mathbf{r} \text{ inside the sample} \tag{34}$$

subject to the appropriate boundary conditions (equivalent equations apply for the **H** field).

The sample shape of lowest symmetry with solutions to Eq. (34) which are independent of **r** is the ellipsoid (i.e. ellipsoidal coordinates are the most general form of separable coordinates for Eq. (34)). In the case of an ellipsoid, the differential equation is called the Lamé equation, and the solutions are the ellipsoidal harmonics [18, 19]. The ellipsoidal coordinates are related to the Cartesian dimension through the elliptic functions of the first and second kind [14]. While solving the problem for an ellipsoid is appealing due to its generality, the solution is quite elaborate and cannot be expressed in terms of classical algebraic functions. Therefore, we will proceed along a simpler course; first we will solve the problem for a sphere [3, 4, 5], followed by a solution in several limiting cases for a spheroid (an ellipse rotated about a symmetry axis) and finally we will develop an approximation scheme which will enable us to obtain results for a general spheroid.

Depending on the ratio of the skin depth δ to sample size a, one can distinguish two limiting cases.

1. Depolarization Regime: $\hat{k}a \ll 1$ In this limit the fields penetrate uniformly throughout the sample and one can effectively neglect the second term in Eq. (34). The resulting case reduces to a solution of Laplace's equation, just as in a static case, and under these conditions the sample is in the so-called depolarization regime.

2. Skin Depth Regime: $\hat{k}a \gg 1$ In this, the skin depth regime, $\hat{k}$ cannot be neglected, and one must solve the full set of Helmholtz equations. However, as we are not interested in the field distribution within the sample, we can use simple arguments to learn about the form of the solution.

The power absorbed is given by the time averaged energy flux of the Poynting vector through the surface of the sample

$$\langle \mathcal{S} \rangle = \frac{c_o}{8\pi} \mathbf{E}_{||} \times \mathbf{H}_{||}^{\star} = -\frac{c_o}{8\pi} \hat{Z}_s |\mathbf{H}_{||}|^2 \hat{e}, \tag{35}$$

where $\mathbf{E}_{||}$ and $\mathbf{H}_{||}$ are the electric and magnetic fields respectively, in the plane of the surface and $\hat{e}$ is a unit vector along the outward normal to the surface. For a good conductor, $\mathbf{E}_{||}$ and $\mathbf{H}_{\perp} \to 0$, while $\mathbf{E}_{\perp}$ and $\mathbf{H}_{||}$ is proportional to the external electric and magnetic fields, respectively (the factor depends solely on the sample geometry). In both cases, the loss is caused by the induced eddy-currents of an effective surface current density

$$\mathbf{K}_{||} = \frac{c_o}{4\pi}\hat{e} \times \mathbf{H}_{||}. \tag{36}$$

The current is proportional to the external field, independent of the sample conductivity (current-driven excitation), and thus, in all cases, the loss is proportional to $\hat{Z}_s$ (i.e. $\Delta \langle W \rangle / \langle W \rangle \propto \hat{Z}_s$).

As shown in Eq. (25), the energy dissipated in the sample is responsible for the variation of the complex frequency of the resonator. If we refer to the perturbation $\Delta\hat{\omega}$ (the variation caused by the introduction of the sample in the empty cavity), we have to include a *real* additive constant, $\lim_{|\hat{\sigma}|\to\infty} \Delta\hat{\omega}/\omega_o$, that represents the shift of the resonance frequency caused by the excluded volume of the field as the body tends to the perfect conductor limit. This offset is called the metallic shift and it depends on the volume, geometry and position (within the resonator) of the sample. For a sample in the skin depth regime, $\Delta\hat{\omega}$ is simply related to the surface impedance

$$\frac{\Delta\hat{\omega}}{\omega_o} = \xi\hat{Z}_s + \lim_{|\hat{\sigma}|\to\infty} \frac{\Delta\hat{\omega}}{\omega_o}, \tag{37}$$

where ξ is the so-called resonator constant. In general, ξ and $\lim_{|\hat{\sigma}|\to\infty} \Delta\hat{\omega}/\omega_o$ depend on the detailed size and shape of the sample under investigation and one must await an appropriate solution of Eq. (33) in order to determine them. However, from very general arguments, we have been able to determine the appropriate form of an equation which relates an experimentally measurable quantity $\Delta\hat{\omega}/\omega_o$ to an intrinsic quantity $\hat{Z}_s$. In fact, provided one knows certain properties of the material under investigation (e.g. it is a good metal with $\delta \ll a$), Eq. (37) is enough to determine normalized values of $\hat{Z}_s$.

To ease the notation, we define a new variation

$$\frac{\Delta'\hat{\omega}}{\omega_o} \equiv \xi\hat{Z}_s = \frac{\Delta\hat{\omega}}{\omega_o} - \lim_{|\hat{\sigma}|\to\infty} \frac{\Delta\hat{\omega}}{\omega_o}, \tag{38}$$

where $\Delta'\hat{\omega}/\omega_o$ is the complex frequency shift from a perfectly conducting body of the same size and shape as the sample. Equating the real and

imaginary parts of Eq. (38) gives

$$\Delta'\Gamma = \Delta\Gamma, \tag{39}$$

$$\Delta' f = \Delta f - \lim_{|\hat{\sigma}|\to\infty} \Delta f. \tag{40}$$

$\Delta' f/f_o$ will be hereafter be referred to as the shift from a perfect conductor.

4 Solutions of the Helmholtz Equation

4.1 The Sphere

We are looking for a solution of the Helmholtz equation that depends only on the external field $\mathcal{E}$ or $\mathcal{H}$. We will first solve the problem of a sphere in a magnetic field. Following Landau [3], we seek a solution (inside the sample) of the form $\mathbf{A} = \beta\nabla \times (s\mathcal{H})$, where $\mathbf{A}$ is the vector potential (polar) and $\mathbf{H} = \nabla \times \mathbf{A}$ is the magnetic field. s is the spherically symmetrical solution of the scalar equation $\nabla^2 s + \hat{k}^2 s = 0$ and β is a constant which depends on the boundary conditions. The only solution (finite at $r = 0$) of this differential equation is the zero$^{\text{th}}$ order spherical Bessel function, $s = j_o(\hat{k}r)$. The solution of the differential equation exterior to the sample (Laplace's Equation) gives an external field $\mathbf{H}$ which is the sum of the applied field $\mathcal{H}$ and the induced dipole field $\hat{\alpha}\mathcal{H}$. By matching the boundary conditions, we compute the polarizability $\hat{\alpha}$ of the specimen

$$\hat{\alpha} = \frac{1}{4\pi}\frac{n}{n-1}\left(1 - \frac{x j_1(x)}{n\partial[x j_1(x)]/\partial x}\right)_{x=\hat{k}a}, \tag{41}$$

where $n = 1/3$ (the depolarization factor of a sphere), $-j_1(x)/2 = j_o'(x)$ is the first derivative of the zero$^{\text{th}}$ order spherical Bessel function and a is the radius of the sphere.

This form of the solution is also valid for the electric field (in the quasi-static limit), and one can therefore write

$$\mathbf{P} = \hat{\alpha}_e \mathcal{E} = \frac{3}{4\pi}\frac{\hat{\epsilon}_{\text{eff}} - 1}{\hat{\epsilon}_{\text{eff}} + 2}\mathcal{E}, \tag{42}$$

and

$$\mathbf{M} = \hat{\alpha}_m \mathcal{H} = \frac{3}{4\pi}\frac{\hat{\mu}_{\text{eff}} - 1}{\hat{\mu}_{\text{eff}} + 2}\mathcal{H}. \tag{43}$$

where, following Champlin and Krongard [4], we have expressed the result in the form of the Clausius-Mossotti equation [12]. The effective permeability $\hat{\mu}_{\text{eff}}$ and permittivity $\hat{\epsilon}_{\text{eff}}$ are given by

$$\hat{\mu}_{\text{eff}} = \hat{\beta}\hat{\mu} \tag{44}$$

$$\hat{\epsilon}_{\text{eff}} = \hat{\beta}\hat{\epsilon}, \tag{45}$$

where in each case $\hat{\beta}$ is given by

$$\hat{\beta} = -2\left(\frac{-(\hat{k}a)\cos(\hat{k}a) + \sin(\hat{k}a)}{-(\hat{k}a)\cos(\hat{k}a) + \sin(\hat{k}a) - (\hat{k}a)^2\sin(\hat{k}a)}\right). \tag{46}$$

Using Eq. (32), we obtain

$$\frac{\Delta\hat{\omega}}{\omega_o} = -\frac{\gamma}{n}\,\frac{\hat{\epsilon}_{\text{eff}} - 1}{\hat{\epsilon}_{\text{eff}} + 2} \tag{47}$$

in the electric field. The result in the magnetic field is obtained by merely substituting $\hat{\mu}_{\text{eff}}$ for $\hat{\epsilon}_{\text{eff}}$ [20].

The following recipe gives the procedure used to extract $\hat{\epsilon}$:

1. Substituting Eqs. (44) or (45) into Eq. (47), one can rewrite it in the form

$$\left.\frac{\Delta\hat{\omega}}{\omega_o}\right|_E = \mathcal{F}_E(\hat{\mu}, \hat{\epsilon}) \tag{48}$$

$$\left.\frac{\Delta\hat{\omega}}{\omega_o}\right|_H = \mathcal{F}_H(\hat{\mu}, \hat{\epsilon}), \tag{49}$$

   where $\mathcal{F}_{E,H}$ represents the functional dependence (generally different in the E and H fields) on $\hat{\mu}$ and $\hat{\epsilon}$, and $\left.\frac{\Delta\hat{\omega}}{\omega_o}\right|_{E,H}$ are the measured shifts in the electric and magnetic field respectively.

2. Inverting these functions $\mathcal{F}_{E,H}$ and equating real and imaginary parts one can solve for both $\hat{\mu}$ and $\hat{\epsilon}$. Note, in most cases, $\mu_{dc} = 1$, so that a measurement in *either* the electric or magnetic field is sufficient to determine $\hat{\epsilon}$.

One result obtained from this analysis is that a non-magnetic sample (μ_{dc}=1) has a non-zero high-frequency magnetic polarizability that depends on the conductivity of the material.

$\hat{\beta}$ tends to a simple limiting value when $|\hat{k}a| \ll 1$ or $|\hat{k}a| \gg 1$:

$$\lim_{\hat{k}a \to 0} \hat{\beta} = 1 + \frac{1}{10}(\hat{k}a)^2 + \frac{9}{700}(\hat{k}a)^4 + \mathcal{O}[(\hat{k}a)^6], \tag{50}$$

$$\lim_{\sigma_1 \to \infty} \hat{\beta} = \frac{2i}{\hat{k}a}. \tag{51}$$

4.2 Sphere in the Electric Field Maximum

Inverting the normal procedure, we have computed $\Delta'\hat{\omega}/\omega_o = \Delta' f/f_o + \mathrm{i}\,\Delta'\Gamma/2f_o$ for a sphere ($n = 1/3$) in the electric field as a function of $n\epsilon_2$, with $\epsilon_1 = 1$. The results are displayed in Fig. 1 and we note the following features:

a. the absorption $\Delta\Gamma$ peaks when $\epsilon_1 = \epsilon_2 + 1 - 1/n$.

b. the metallic shift ($\lim_{|\hat{\sigma}| \to \infty} \Delta\hat{\omega}/\omega_o$) is equal to $-\gamma/n$ (note the sign).

c. the shift $\Delta' f/f_o$ changes sign and becomes negative in the skin depth regime.

On Fig. 2 we have replotted $\Delta\Gamma/2f_o$ and $|\Delta' f/f_o|$ (normalized to the metallic shift (γ/n)) on a logarithmic scale to emphasize that, in the skin depth regime, $\Delta\Gamma/2f_o$ and $\Delta' f/f_o$ are both equal and proportional to the surface impedance ($\propto 1/\sqrt{\epsilon_2}$). On this plot $\Delta' f/f_o$ changes sign at the position of the logarithmic divergence.

We observe three independent regimes, each of which are characterized by a different power law dependence of the loss $\Delta\Gamma$:

1. $\epsilon_2 < \epsilon_1 - 1 + 1/n$, this is the insulating side of the depolarization regime. In this range, $\Delta\Gamma/2f_o \propto \sigma_1$ and the frequency shift saturates to a constant (which is proportional to ϵ_1).

2. $\epsilon_1 - 1 + 1/n < \epsilon_2 < 4\pi(c_o/\omega a)^2$, this is the metallic side of the depolarization regime, where the skin depth ($\delta = (c_o/\omega)\sqrt{2/\epsilon_2}$) is still larger than the radius of the sphere (a) but with the restriction $\epsilon_2 > \epsilon_1/n$. In this regime $\Delta\Gamma/2f_o \propto 1/\sigma_1$ and the frequency shift goes asymptotically to the metallic shift from *below*.

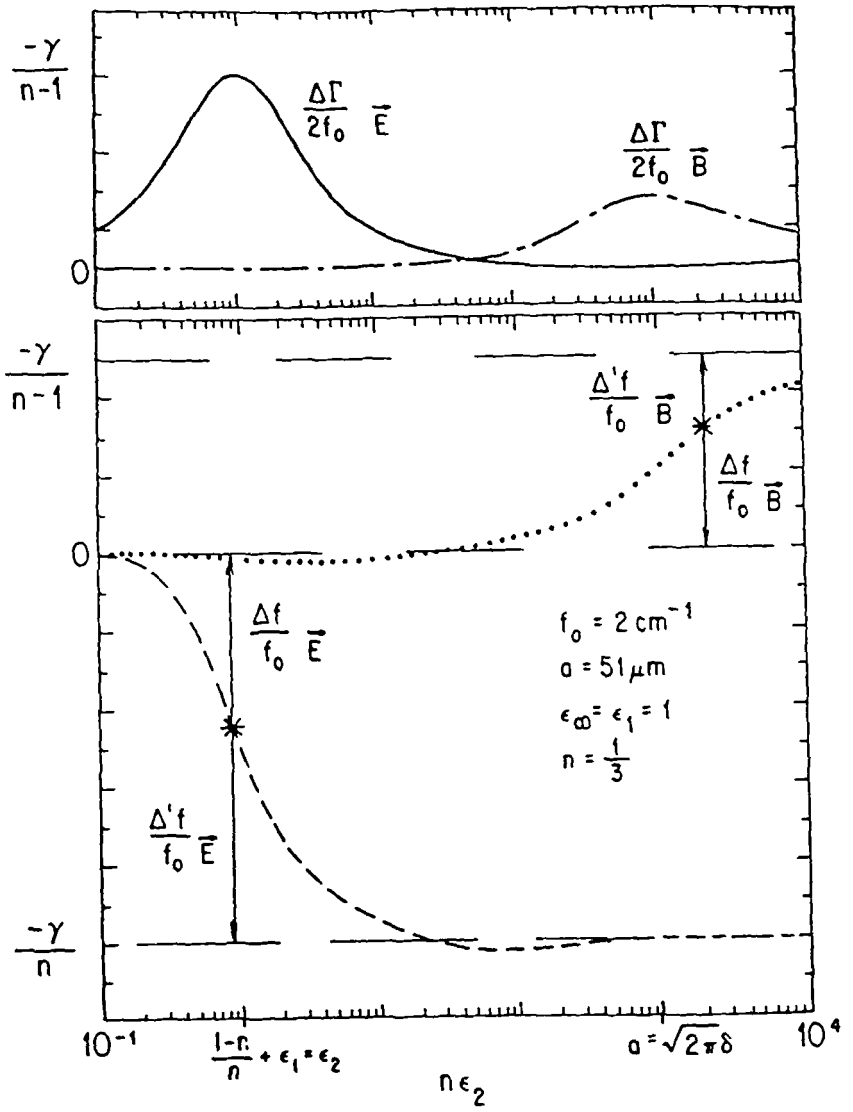

Figure 1: *The ϵ_2 dependence of $\Delta\hat{\omega}/\omega$ for a sphere of radius $a = 51$ μm in the electric or magnetic field antinode ($\epsilon_1 = 1$). Δf is the frequency shift, and $\Delta' f$ is the shift from a perfect conductor. The metallic shift ($lim_{|\hat{\sigma}|\to\infty}\Delta\hat{\omega}/\omega_o$) is equal to $-\gamma/n$ in the* **E** *field and $-\gamma/(n-1)$ in the* **H** *field. Notice that $\Delta f/f_o$ changes sign in the magnetic field when $\Delta' f/f_o$ does so in the electric field.*

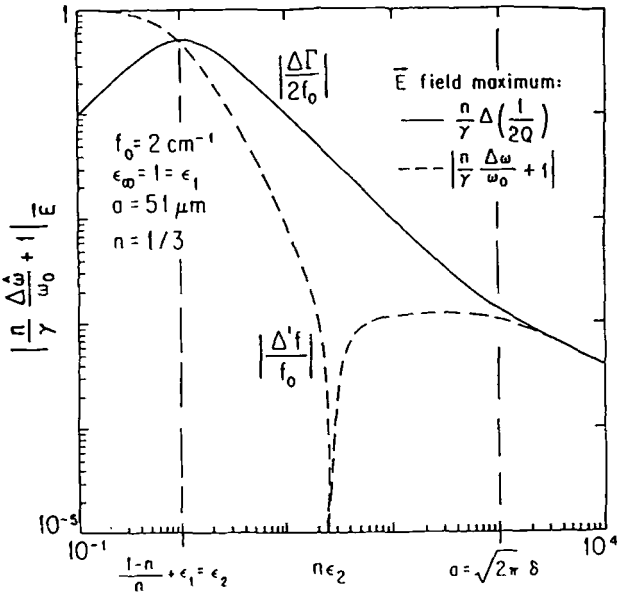

Figure 2: *The ϵ_2 dependence of the absolute value of $\Delta\Gamma$ and $\Delta' f$ for a sphere of radius $a = 51\mu m$ in the electric field maximum at f=2 cm^{-1} ($\epsilon_1 = 1$). We observe three distinct regimes, each characterized by a different power law dependence of the loss $\Delta\Gamma$. In the skin depth regime (far right), $\Delta\Gamma = -\Delta' f \propto \sqrt{1/\epsilon_2}$ and $\Delta'\hat{\omega}/\omega_o$ is proportional to the surface impedance. The frequency shift $\Delta f/f_o$ is always negative, but the shift from a perfect conductor $\Delta' f/f_o = \Delta f/f_o + \gamma/n$ changes sign near $n\epsilon_2 = 20$, at the point of the negative divergence.*

3. $4\pi(c_o/\omega a)^2 < \epsilon_2$, this is the skin depth regime. In this regime, $\Delta\Gamma/2f_o \sim -\Delta' f/f_o \propto 1/\sqrt{\sigma_1}$ as shown in Fig. 2, thus demonstrating that $\Delta'\hat{\omega}/\omega_o = \xi\hat{Z}_s$, as predicted by Eq. (38). Using the fact that $\lim_{\sigma_1\to\infty}\hat{\beta} = 2i/\hat{k}a$, we can expand Eq. (47) to obtain

$$\lim_{\sigma_1\to\infty}\frac{\Delta\hat{\omega}}{\omega_o} \sim -\frac{\gamma}{n}\left(1+\frac{i\hat{k}a}{2n\hat{\epsilon}}\right) = -\frac{\gamma}{n}+\xi\hat{Z}_s, \tag{52}$$

where the resonator constant ξ is given by

$$\xi = \frac{-i\gamma}{n^2}\left(\frac{\omega a}{2c_o}\right) = -\frac{9}{2}\,i\gamma\,\frac{\omega a}{c_o}, \tag{53}$$

and the metallic shift is

$$\lim_{|\hat{\sigma}|\to\infty} \frac{\Delta\hat{\omega}}{\omega_o} = -\frac{\gamma}{n}. \tag{54}$$

4.2.1 Sphere in the Magnetic Field Maximum

Using the same procedure as in the electric field, we have computed $\Delta'\hat{\omega}/\omega_o$ for a sphere in the maximum of the magnetic field. The results are displayed in Fig. 1 and we observe several differences from the results obtained in the electric field; namely

a. the absorption, $\Delta\Gamma$, peaks when $\sqrt{2\pi}\ a = \delta$.

b. the metallic shift ($\lim_{|\hat{\sigma}|\to\infty} \Delta\hat{\omega}/\omega_o$) is positive and equal to $-\gamma/(n-1)$ (a metal has a finite frequency polarizability that is positive in the electric field and negative in the magnetic field).

c. the frequency shift $\Delta f/f_o$ changes sign and becomes positive in the skin depth regime.

We have plotted the absolute value of the results on a logarithmic scale in Fig. 3 and in contrast to the results found in the electric field, we find only two independent regimes:

1. $4\pi(c_o/\omega a)^2 > \epsilon_2$, this is the depolarization regime, where the magnetic field penetrates throughout the sample. We observe that $\Delta\Gamma/2f_o \propto \sigma_1$ and the frequency shift Δf saturates to a constant (approximately zero for a metal).

2. $4\pi(c_o/\omega a)^2 < \epsilon_2$, this is the skin depth regime, and the magnetic field is expelled from the sample (diamagnetism). Furthermore, $\Delta\Gamma/2f_o = -\Delta' f/f_o \propto 1/\sqrt{\epsilon_2}$, and is thus proportional to the surface impedance (cf. Eq. (14)). As before, we find

$$\lim_{\sigma_1\to\infty} \frac{\Delta\hat{\omega}}{\omega_o} \sim -\frac{\gamma}{n-1}\left(1 + \frac{2i}{\hat{k}a(n-1)}\right) = -\frac{\gamma}{n-1} + \xi\hat{Z}_s. \tag{55}$$

In the magnetic field, the resonator constant of a sphere is

$$\xi = \frac{-i\gamma}{(n-1)^2}\left(\frac{2c_o}{\omega a}\right) = -\frac{9}{2}\, i\gamma\, \frac{c_o}{\omega a}, \tag{56}$$

while the metallic shift is given by

$$\lim_{|\hat{\sigma}|\to\infty} \frac{\Delta\hat{\omega}}{\omega_o} = -\frac{\gamma}{n-1}. \tag{57}$$

In the inset of Fig. 3 we have plotted $\Delta f/f_o$ to show the change of sign of the frequency shift. We have assumed that the permeability of the material is 1 (generally the case for a metal [3]).

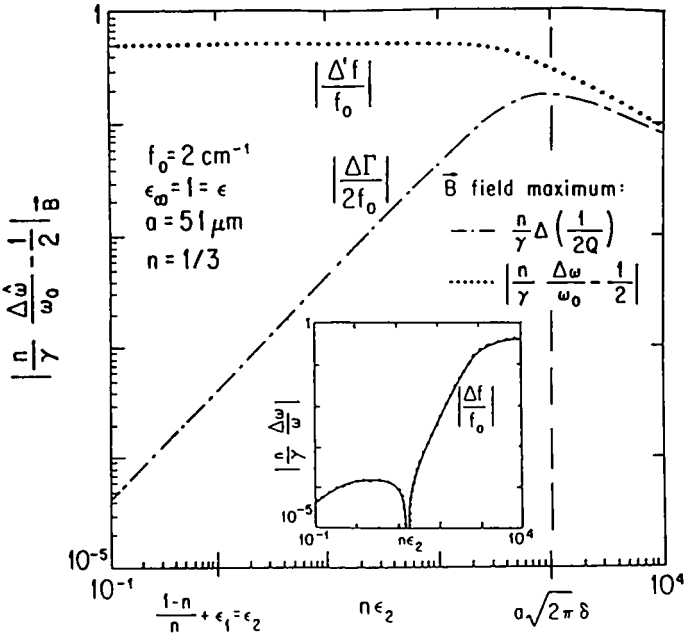

Figure 3: *The ϵ_2 dependence of the absolute value of $\Delta\Gamma$ and $\Delta' f$ for a sphere of radius $a = 51\ \mu m$ in the magnetic field maximum at $f = 2\ cm^{-1}$ (ϵ_1=1). In the inset we show the dependence of the frequency shift $\Delta f/f_o$. We observe two distinct regimes, each characterized by a different power law dependence of the loss $\Delta\Gamma$. In the skin depth regime (far right) $\Delta\Gamma = -\Delta' f \propto \sqrt{1/\epsilon_2}$ and $\Delta'\hat{\omega}/\omega_o$ is proportional to the surface impedance. The shift from a perfect conductor $\Delta' f/f_o$ is always negative, but the frequency shift $\Delta f/f_o = \Delta' f/f_o - \gamma/(n-1)$ changes sign near $n\epsilon_2 = 20$, becoming positive at the point of negative divergence (see inset).*

4.2.2 Comparison with Results of a Drude Metal

In Figs. 2 and 3 we plotted both the real and imaginary parts of $\Delta\hat{\omega}$ as a function of ϵ_2, with ϵ_1 held constant, for the case of a spherical sample. It should be noted that this plot does not conserve the spectral weight of the real part of the conductivity [21, 12]

$$\int_0^\infty \sigma_1(\omega)d\omega = \frac{{\omega_p}^2}{8}. \tag{58}$$

A more realistic solution of Eq. (29) would take in account the fact that σ_1 and σ_2 do not vary independently.

The simplest picture that respects the f-sum rule of Eq. (58) is the Drude model. The permittivity $\hat{\epsilon}$ depends only on four parameters [21]: the plasma frequency ω_p (or the spectral weight), the relaxation rate $1/\tau$, the measurement frequency ω and the permittivity at high frequency ϵ_∞:

$$\sigma_1 = \frac{{\omega_p}^2}{4\pi}\frac{\tau}{1+(\omega\tau)^2}\ ; \quad \sigma_2 = \frac{{\omega_p}^2}{4\pi}\frac{\omega\tau^2}{1+(\omega\tau)^2}, \tag{59}$$

$$\epsilon_1 = \epsilon_\infty - \frac{{\omega_p}^2\tau^2}{1+(\omega\tau)^2}\ ; \quad \epsilon_2 = \frac{{\omega_p}^2\tau/\omega}{1+(\omega\tau)^2}. \tag{60}$$

In the following we will calculate both the frequency and relaxation rate dependence of $\Delta'\hat{\omega}/\omega_o$ for a sphere of radius a with a Drude conductivity.

The parameters used in the example to be discussed are kept constant and are close to experimental values. The radius of the sphere is $a = 51\ \mu$m, the plasma frequency $\omega_p/2\pi$= 1,000 cm^{-1} and the high frequency permittivity $\epsilon_\infty = 1$. When calculating the frequency dependence, the relaxation rate is fixed to $1/2\pi\tau = 1$ cm^{-1} and when calculating the relaxation rate dependence, the excitation frequency is fixed to $f = 2$ cm^{-1} or 60 GHz.

Fig. 4 displays the frequency dependence of the Drude conductivity, while the inset shows the permittivity. Using a logarithmic scale on the inset constrains us to take the absolute value; ϵ_1 is negative below the plasma frequency ($\omega < \omega_p$) and saturates to ϵ_∞ at higher frequency ($\omega > \omega_p$) (ϵ_2 is positive for all frequencies). Notice that ϵ_1 equals zero at the plasma frequency and thus leads to a negative divergence on a logarithmic scale at ω_p (since $\epsilon_\infty = 1$).

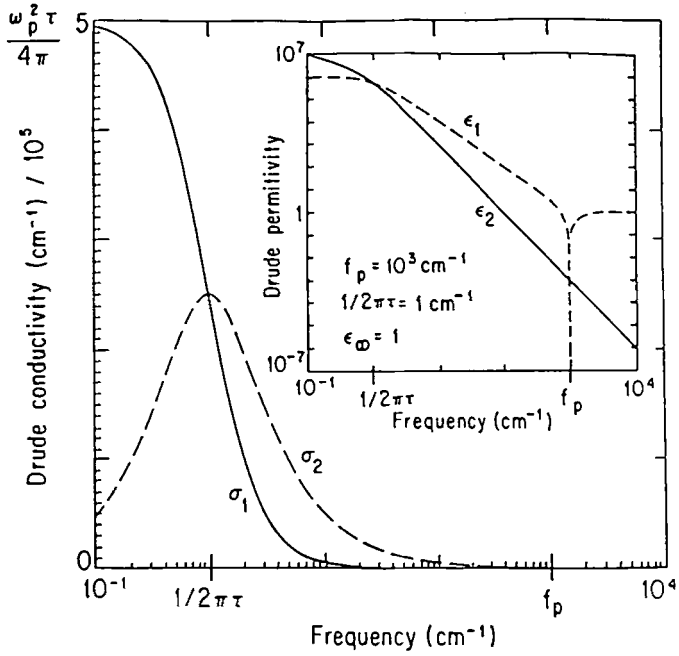

Figure 4: *The frequency dependence of the Drude conductivity (Eq. (59)) with* $1/(2\pi\tau) = 1$ cm^{-1} *and* $\omega_p/2\pi = 1000$ cm^{-1}. *In the inset we display the absolute value of the permittivity on a logarithmic scale. The negative divergence signals the change in sign of* ϵ_1.

In Fig. 5 we display the relaxation rate dependence of a Drude conductivity (the permittivity is proportional since the frequency is kept constant). σ_1 increases as $1/\tau$ for $\omega\tau > 1$ (clean limit) and decreases as τ for $\omega\tau < 1$ (dirty limit). σ_2 is independent of the relaxation rate in the clean limit but is proportional to τ^2 in the dirty limit.

Figs. 6a and b compare the frequency dependence of the Drude surface impedance with $\Delta'\tilde{\omega}/\omega_o$ in both field configurations. We have renormalized $\Delta'\tilde{\omega}/\omega_o$ by the resonator constant. We observe that in the skin depth regime ($\delta \ll a$) $\Delta'\tilde{\omega}/\omega_o$ coincides with the Drude surface impedance up to 100 cm^{-1}. Above this range the free space wavelength c_o/f becomes comparable to the size of the sample and thus we deviate from the quasi- static approximation. Notice on both figures, that in the so-called Hagen-Rubens limit ($\omega\tau \ll 1$), the surface resistance is equal to the surface reactance and they deviate only

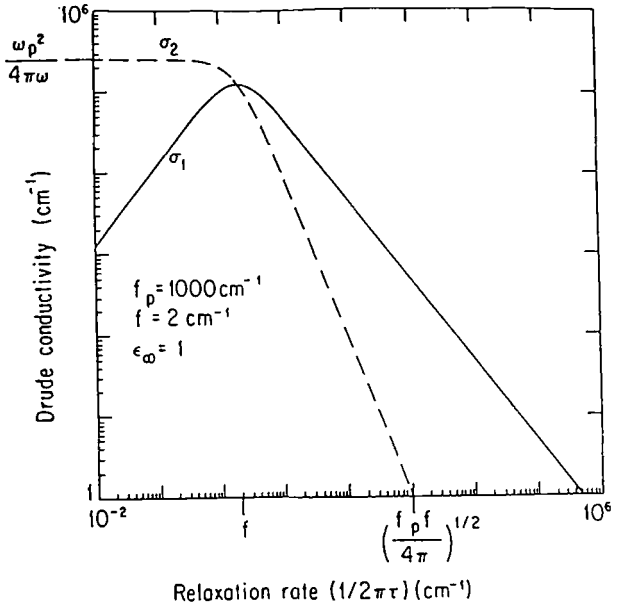

Figure 5: *The relaxation rate dependence of the Drude conductivity at* $\omega_o/2\pi$=2 cm^{-1}, *assuming a plasma frequency* $\omega_p/2\pi$ = 1000 cm^{-1}.

when $\omega\tau$ becomes larger than 1. Outside the skin depth regime ($\delta > a$) the surface impedance no longer has any meaning.

Figs. 7a and b compare the relaxation rate dependence of the surface impedance with the calculation of $\Delta'\tilde{\omega}/\omega_o$ for a sphere in the maximum of **E** or **H**. We have used the same normalization as in the frequency dependence. We observe that in the skin depth regime ($\delta \ll a$) the surface impedance follows the corresponding component of $\Delta\tilde{\omega}/\omega_o$ in both configurations, furthermore in the Hagen-Rubens limit they are all equal. Once again we would like to emphasize the point that when $\delta > a$ the surface impedance no longer has any meaning and $\Delta'\tilde{\omega}/\omega_o$ should not follow the Drude surface impedance. The infinite branch in the electric field configuration is due to the fact that the frequency shift approaches the metallic shift from below and thus crosses the axis of the abscissa.

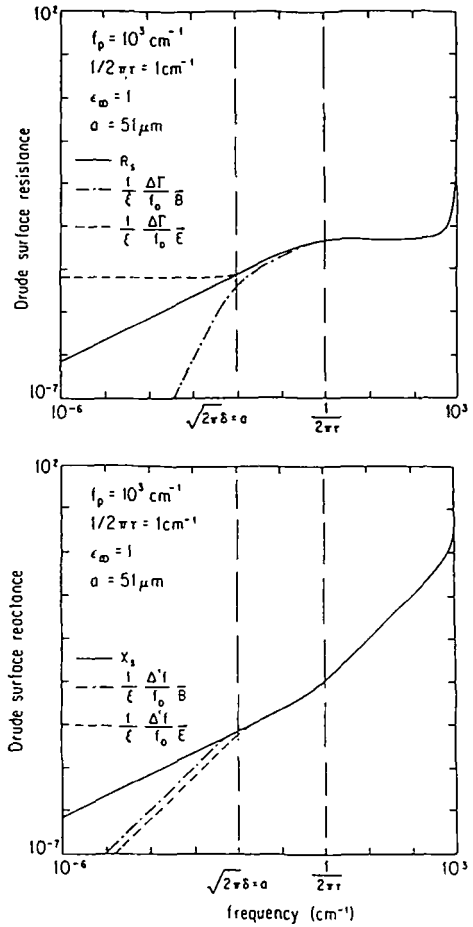

Figure 6: a) *The frequency dependence of the surface resistance* R_s *compared with the absolute value of the half-width* $\Delta\Gamma$ *for a sphere in either the electric or magnetic field antinode. We display* $\Delta\Gamma/2f_o\xi$, *where* ξ *is the resonator constant (given in Table 2), and we observe three regimes*

- $\delta \gg a$ *[left of* $(2\pi)^{1/2}\delta = a$*], this is the depolarization regime and the surface impedance has no meaning*
- $\delta \ll a$ *[right of* $(2\pi)^{1/2}\delta = a$*], this is the skin depth regime and* $\Delta'\hat{\omega}/\omega_o$ *is simply proportional to the surface impedance. If* $\omega\tau \ll 1$, $R_s = X_s$ *and this is the so-called Hagen-Rubens regime. If* $\omega\tau \gg 1$, $X_s > R_s$ *and this is the clean limit.*

b) *The frequency dependence of the surface reactance. As in part* a), *the same three regimes are defined.*

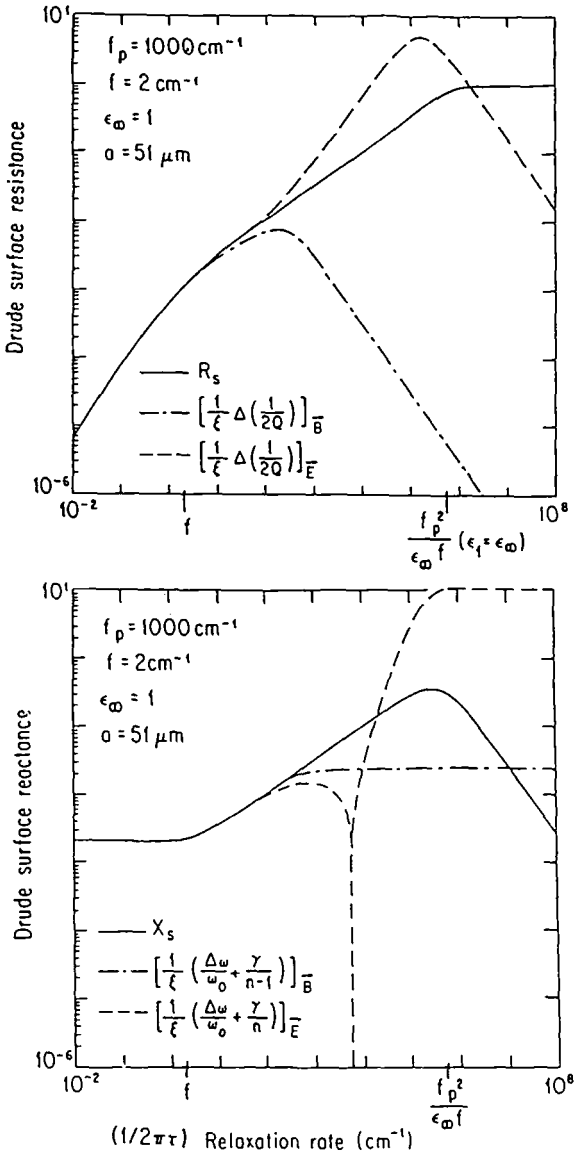

Figure 7: *The relaxation rate dependence of a) the surface resistance R_s and b) the surface reactance X_s compared with the absolute value of the half-width $\Delta\Gamma$ for a sphere in either the electric or magnetic field antinode. Again, we display $\Delta\Gamma/2f_o\xi$ and observe the same three regimes as in Fig. 6.*

4.3 The Spheroid

4.3.1 Exact Solutions

To our knowledge, the relationship between $\hat{\sigma}$ and $\Delta\hat{\omega}/\omega_o$ for a general spheroid of arbitrary conductivity has never been calculated. However, a variety of solutions have been presented in different limits [6, 7, 8]. We will present the results of the calculations that have been made in the various limits and expand on some of these results.

Depolarization Regime: $\hat{k}a \gg 1$ For a poorly conducting compound the external fields penetrate throughout the sample and a simple analysis is possible.

- Electric Field: In the electric field antinode, the field inside the sample can be determined using Eqs. (6) and (8), with

$$\mathbf{E} = \frac{\mathcal{E}}{1 + n(\hat{\epsilon} - 1)}, \tag{61}$$

where n is the depolarization factor along the external field direction. Replacing $\mathcal{E}$ with the value in Eq. (10), and rearranging one finds

$$\hat{\alpha}_e = \frac{1}{4\pi} \frac{\hat{\epsilon} - 1}{1 + n(\hat{\epsilon} - 1)}. \tag{62}$$

The real and imaginary components of Eq. (29) give

$$\frac{1}{2}\left(\frac{1}{Q_s} - \frac{1}{Q_o}\right) = \gamma \frac{\epsilon_2}{[1 + n(\epsilon_1 - 1)]^2 + (n\epsilon_2)^2}, \tag{63}$$

$$\frac{f_s - f_o}{f_o} = -\gamma \frac{(\epsilon_1 - 1)[1 + n(\epsilon_1 - 1)] + n{\epsilon_2}^2}{[1 + n(\epsilon_1 - 1)]^2 + (n\epsilon_2)^2}, \tag{64}$$

as first derived by Buranov and Shchegolev [6].

Taking the limit $|\hat{\epsilon}| \gg 1$ in the previous equation, one finds that the electric polarizability tends to a positive constant

$$\hat{\alpha}_e = \frac{1}{4\pi n}\left(1 - \frac{1}{n\hat{\epsilon}} + \frac{1 - n}{(n\hat{\epsilon})^2} + \mathcal{O}\left[\frac{1}{\hat{\epsilon}}\right]^3\right) \tag{65}$$

and

$$\frac{1}{2}\left(\frac{1}{Q_s}-\frac{1}{Q_o}\right) = \gamma\frac{\epsilon_2}{|n\hat{\epsilon}|^2}+\mathcal{O}\left[\frac{1}{\hat{\epsilon}}\right]^2, \tag{66}$$

$$\frac{f_s-f_o}{f_o} = \frac{-\gamma}{n}+\gamma\frac{\epsilon_1}{|n\hat{\epsilon}|^2}+\mathcal{O}\left[\frac{1}{\hat{\epsilon}}\right]^2. \tag{67}$$

- Magnetic Field: In the limit $\hat{k}a \ll 1$ the magnetic polarizability is computed from Eq. (62), but with the permittivity $\hat{\epsilon}$ replaced by the permeability $\hat{\mu}$. Thus, in the magnetic field one determines the complex permeability $\hat{\mu}$ from the measured $\Delta\hat{\omega}$. However, even though the dc permeability of a non-magnetic metal $\mu_{\rm dc}=1$, at finite frequencies the magnetic polarizability is finite. (The same is also true for a purely magnetic material in the electric field i.e. provided $\hat{\mu}\neq 1$, $\hat{\alpha}_e \neq 0$ in an ac field even though $\hat{\epsilon}$=1.) Unfortunately, the magnetic polarizability depends on the geometry of the sample and it is difficult to calculate. To a first approximation, it is given by

$$\hat{\alpha}_m = \frac{1}{40\pi}\frac{(\hat{k}a)^2}{\varsigma}, \tag{68}$$

where ς is a constant that depends on the geometry of the sample ($\varsigma=1$ for a sphere). As discussed previously, this effect is due to the finite conductivity.

Skin Depth Limit: $\hat{k}a \gg 1$ In the skin depth limit, the fields are not constant within the sample and the calculations are considerably more difficult.

- Electric Field Maximum: A computation for a prolate spheroid ($a > b = c$) in the skin depth regime has been performed by Cohen and Ong [7, 8]. They computed the resonator constant ξ for a prolate spheroid of eccentricity $\varepsilon = \sqrt{1-(b/a)^2}$ in the limit $a \gg b$ and obtained

$$\mathrm{Im}\left(\frac{\Delta\hat{\omega}}{\omega_o}\right) = \mathrm{Im}(\xi\hat{Z}_s), \tag{69}$$

where

$$\xi = -i\frac{9\pi}{2^5}\frac{\gamma}{n^2}\left(\frac{\omega b}{2c_o}\right), \tag{70}$$

and n is the depolarization factor along the field.

Table 2: *Resonator constant ξ of a spheroid for different orientations in either the electric or magnetic field antinode, where $2a \gg 2b$ are the sample dimensions, c_o the speed of light, n the depolarization factor, $\omega/2\pi$ the measurement frequency, ξ_{sphere} the resonator constant of a sphere enclosing the sample (radius a), $\hat{z}$ is the direction of the spheroid symmetry axis and the field is either parallel or perpendicular to this symmetry axis.*

Resonator Constant			
		Electric Field	Magnetic Field
Sphere	All Fields	$-i\gamma/n^2$ $[\omega a/2c_o]$	$-i\gamma/(n-1)^2$ $[2c_o/\omega a]$
		ξ/ξ_{sphere}	ξ/ξ_{sphere}
Prolate Spheroid	Field $\parallel \hat{z}$	$(3^2\pi/2^5)\, b/a$	$(3\pi/2^3)\, a/b$
	Field $\perp \hat{z}$	$(3\pi^3/2^6)\, b/a$	$(3\pi/2^4)\, a/b$
Oblate Spheroid	Field $\parallel \hat{z}$	$(3/2^3)\, a/b$	$(3/2)\, b/a \ln(a/b)$
	Field $\perp \hat{z}$	$(3^2/2^3)\, b/a \ln(a/b)$	$(3/2^2)\, a/b$

We have extended their calculations to include field orientations both parallel and perpendicular to the semi-major axis for both a prolate and oblate spheroid in the limit $a \gg b$. The results are listed in Table 2.

- Magnetic Field: To the authors' knowledge, the calculations for either a prolate or oblate spheroid have not been made. The calculations are straightforward but somewhat tedious and we have therefore only reproduced the calculation in Appendix C. For a prolate spheroid with $\mathbf{H} \parallel \hat{z}$ in the limit $a \gg b$ (i.e. needle shaped sample) we found

$$\xi = \frac{-3i\gamma c_o \pi}{4b\omega(n-1)^2}. \tag{71}$$

The calculation is similar with the field perpendicular to the symmetry axis as well as for an oblate spheroid, and we therefore simply reproduce the results (in the limit $a \gg b$) in Table 2.

A comparison can be made of the loss when the sample is placed at the maximum of either the electric field or magnetic field. For a prolate spheroid in the limit $a \gg b$, the bulk of the currents run along the a-axis ($\mathbf{E} \parallel \hat{a}$ and $\mathbf{H} \perp \hat{a}$) and one finds

$$\varrho = \frac{\Delta\left(\frac{1}{2Q}\right)_{\mathbf{B}}}{\Delta\left(\frac{1}{2Q}\right)_{\mathbf{E}}} = \frac{2}{3}\frac{{n_{\parallel}}^2}{(1-n_{\perp})^2}\left(\frac{2c_o}{\omega b}\right)^2, \tag{72}$$

where $n_{\parallel}$ and $n_{\perp}$ are the depolarization factors parallel and perpendicular to $\hat{a}$ respectively. Typical values are $a = 575\ \mu\text{m}$, $b = 50\ \mu\text{m}$, and $f = \omega/2\pi = 60 \times 10^9\ \text{s}^{-1}$. Using these values of a and b one finds [14] $n_{\parallel} = .0164$, $n_{\perp} = .4918$, and $\varrho = .71$. As ϱ depends on the geometry of the sample, the relative sensitivity of the measurement can be increased by choosing the appropriate configuration.

4.4 The Spherical Approximation

While the solutions presented above are good for a spheroid in either the skin depth or depolarization regime, large changes take place in the cross-over region and it is not possible to simply extend either solution across this border. This cross-over region is of particular importance for a variety of organic conductors, where the samples are generally small and the temperature dependence of the conductivity large. In particular, the frequency dependent transport is oftentimes of interest in the near vicinity of a metal-insulator transition, and it is at this point where one is most likely to cross-over to the other regime. It is for this reason that we have attempted to approximate the solution for a general spheroid by extending the exact results obtained for a sphere.

Keeping in mind that the Clausius-Mossotti expression was conceived as a first order approximation of the polarizability for a spherically symmetric system, we will define an expression relating the permittivity and the polarizability for an ellipsoid. Defining a generalized Clausius-Mossotti expression

$$\hat{\alpha}_e = \frac{1}{4\pi n}\frac{\hat{\epsilon}_{\text{eff}} - \alpha_1}{\hat{\epsilon}_{\text{eff}} + \alpha_2}, \tag{73}$$

where the effective values are defined by the same formulas as in Eq. (45) and the form of $\hat{\beta}$ from the spherical case will be adopted.

We will now proceed to evaluate this expression in several different limiting cases and to compare with the exact results obtained earlier.

Depolarization Regime: $\hat{k}a \ll 1$ In this limit, $\hat{\beta} \sim 1$ (see Eq. (50)) and therefore $\hat{\epsilon}_{\text{eff}} \sim \hat{\epsilon}$. Equating this expression with Eq. (62) we find

$$\alpha_1 = 1, \tag{74}$$

and

$$\alpha_2 = \frac{1-n}{n}. \tag{75}$$

Inserting these values we obtain the following expressions for the polarizability in the electric

$$\hat{\alpha}_e = \frac{1}{4\pi} \frac{\hat{\beta}\hat{\epsilon} - 1}{1 + n(\hat{\beta}\hat{\epsilon} - 1)} \tag{76}$$

and magnetic fields

$$\hat{\alpha}_m = \frac{1}{4\pi} \frac{\hat{\beta}\hat{\mu} - 1}{1 + n(\hat{\beta}\hat{\mu} - 1)}. \tag{77}$$

Skin Depth Regime: $\hat{k}a \gg 1$ In this case $\hat{\beta} \propto (\hat{k}a)^{-1}$.

- Electric Field: In this limit the effective permittivity $\hat{\epsilon}_{\text{eff}} \to \infty$ and the induced variation of the cavity characteristics are given by

$$\frac{\Delta\hat{\omega}}{\omega_o} = -\frac{\gamma}{n} + \frac{\gamma}{n^2}\frac{1}{\hat{\epsilon}_{\text{eff}}}, \tag{78}$$

to first order in $1/\hat{\epsilon}_{\text{eff}}$. Using Eq. (51) one finds

$$\frac{\Delta\hat{\omega}}{\omega_o} = -\frac{\gamma}{n} + \frac{\gamma}{n^2}\frac{\omega a}{2c_o}(-i)\hat{Z}_{\text{eff}}, \tag{79}$$

where $\hat{Z}_{\text{eff}}$ is proportional to $\hat{Z}_s$. On comparing with Eq. (37) and using the resonator constants from Table 2 one finds

$$\hat{Z}_{\text{eff}} = \frac{\xi}{\xi_{\text{sphere}}}\hat{Z}_s. \tag{80}$$

So, in this limit, we can exactly reproduce the earlier results by including the value of the normalized resonator constant obtained from the exact calculation made in the skin depth limit.

- Magnetic Field: In this case the effective permeability $\hat{\mu}_{\text{eff}} \to 0$ and one finds

$$\frac{\Delta\hat{\omega}}{\omega_o} = \frac{\gamma}{1-n} + \frac{\gamma}{(1-n)^2}\hat{\mu}_{\text{eff}}. \tag{81}$$

Following the same procedure one finds

$$\frac{\Delta\hat{\omega}}{\omega_o} = \frac{\gamma}{1-n} + \frac{\gamma}{(1-n)^2}\frac{2c_o}{\omega a}(-i)\hat{Z}_{\text{eff}}. \tag{82}$$

We are thus able to piece together a solution which is valid for arbitrary values of the conductivity by including the information which was earlier obtained by an exact solution in several limiting cases. While this approach is certainly an over-simplification, it works surprisingly well in the limiting cases. However, the error introduced is difficult to estimate (it certainly depends on the depolarization factor) and the absolute values should not be taken too seriously. Nevertheless, it is a powerful approach and we will present several results obtained in this fashion in Part III of these papers. Finally, we cannot, of course, extend this type of a solution to a sample of arbitrary shape as we must first be able to calculate the correction factor ξ/ξ_{sphere}.

5 Conclusion

In summary, we have established a relationship between the intrinsic conductivity $\hat{\sigma} = \sigma_1 + i\sigma_2$ and the parameters experimentally accessible with the cavity perturbation technique: the frequency shift Δf and the bandwidth $\Delta\Gamma$. We have computed explicitly the result for a sphere and compared it with the calculation of the surface impedance assuming that the conductivity follows a Drude behavior. In the skin depth regime, we have carried out the computation for both a prolate an oblate spheroid at the electric and magnetic field maximum for every possible orientation of the sample with respect to the applied field.

Acknowledgements

We are greatly indebted to Dr. D. Senouf of the UCLA mathematics department for his help in numerical calculations. We also would like to thank Dr. A. Awasthi and Dr. L. Drabeck for useful discussions. This research was partially supported by the INCOR program of the University of California. One of us (M.D.) would like to acknowledge the support of the Alexander von Humboldt-Foundation.

Appendix A. Depolarization Factor

If a, b and c are the sample dimensions along the three principal axes x, y and z respectively, and

$$a \geq b \geq c > 0 \tag{83}$$

then the depolarization factors are given by

$$n_x = \frac{\cos\phi\cos\theta}{k^2\sin^3\theta}\left[F(k,\theta) - E(k,\theta)\right], \tag{84}$$

$$n_y = \frac{\cos\phi\cos\theta}{k^2(1-k^2)\sin^3\theta}\left[E(k,\theta) - (1-k^2)F(k,\theta) - \frac{k^2\sin\theta\cos\theta}{\cos\phi}\right] \tag{85}$$

$$n_z = \frac{\cos\phi\cos\theta}{(1-k^2)\sin^3\theta}\left[\frac{\sin\theta\cos\phi}{\cos\theta} - E(k,\theta)\right], \tag{86}$$

where

$$\cos\phi = \quad b/a, \qquad (0 \leq \phi \leq \frac{\pi}{2}), \tag{87}$$

$$\cos\theta = \quad c/a, \qquad (0 \leq \theta \leq \frac{\pi}{2}), \tag{88}$$

$$k = \quad \sin\phi/\sin\theta. \tag{89}$$

$F(k,\theta)$ and $E(k,\theta)$ are the elliptic integrals of the first and second kind; k is the modulus and θ the amplitude.

A simple relationship exists among the matrix elements of the depolarization tensor; in the principal basis the trace is equal to unity

$$n_x + n_y + n_z = 1. \tag{90}$$

The depolarization factors take on fairly simple forms in several limiting cases:

1. A sphere ($a = b = c$): $n_x = n_y = n_z = 1/3$.
2. A cylinder in the x-direction ($a \to \infty, b = c$): $n_x = 0, n_y = n_z = 1/2$.
3. A flat plate ($a, b \to \infty$): $n_x = n_y = 0, n_z = 1$.
4. A prolate spheroid ($a > b = c$) of eccentricity $\varepsilon = \sqrt{1-(b/a)^2}$

$$n_x = \frac{1-\varepsilon^2}{2\varepsilon^3}\left(\ln\frac{1+\varepsilon}{1-\varepsilon} - 2\varepsilon\right), \quad n_y = n_z = \tfrac{1}{2}(1-n_x). \tag{91}$$

5. An oblate spheroid ($a = b > c$) with $\varepsilon = \sqrt{(a/c)^2 - 1}$

$$n_z = \frac{1+\varepsilon^2}{\varepsilon^3}(\varepsilon - \arctan\varepsilon), \quad n_x = n_y = \tfrac{1}{2}(1 - n_z). \tag{92}$$

6. A prolate ellipsoid ($a \gg b \geq c$)

$$n_x = \frac{bc}{a^2}\left(\ln\left(\frac{4a}{b+c}\right) - 1\right). \tag{93}$$

B. TE_{011} Cylindrical Cavity

For a cylindrical cavity of radius $d/2$ and height h, resonating at the TE_{011} mode, the fields inside the cavity are given by

$$H_r(r,z) = \frac{H_o J_o'(kr)\cos\left(\frac{\pi z}{h}\right)}{\sqrt{1+\left(\frac{2\alpha_{01}h}{\pi d}\right)^2}}, \tag{94}$$

$$H_z(r,z) = \frac{H_o J_o(kr)\sin\left(\frac{\pi z}{h}\right)}{\sqrt{1+\left(\frac{\pi d}{2\alpha_{01}h}\right)^2}}, \tag{95}$$

$$E_\phi(r,z) = -\sqrt{\frac{\mu}{\epsilon}} H_o J_o'(kr)\sin\left(\frac{\pi z}{h}\right), \tag{96}$$

$$E_r(r,z) = H_\phi = E_z = 0, \tag{97}$$

where J_o', represents the derivative of the zero$^{\text{th}}$ order cylindrical Bessel function, $k = 2\alpha_{01}/d$, and $\alpha_{01} = 3.83171$. The frequency of the cavity is given by

$$\omega_o = c_o\sqrt{\left(\frac{2\alpha_{01}}{d}\right)^2 + \left(\frac{\pi}{h}\right)^2} = 2\pi f_o. \tag{98}$$

while the average of the electric field is

$$\lhd|\mathcal{E}|^2\rhd = 0.0832\frac{\mu}{\epsilon}H_o^2. \tag{99}$$

The electric field antinode occurs at

$$r = 0.481a. \tag{100}$$

For a cavity of dimension $d/h = 3/2$, the mode constant is

$$\gamma_o = \begin{cases} 2.03 & \text{at } r = 0.48d/2 \text{ and } z = h/2 \quad \text{Electric Field,} \\ 0.675 & \text{at } r = 0.48d/2 \text{ and } z = 0 \quad \text{Magnetic Field} \\ 4.18 & \text{at } r = 0 \text{ and } z = h/2 \quad \text{Magnetic Field.} \end{cases} \tag{101}$$

C. Resonator Constant of a Prolate Spheroid in the Magnetic Field

If the sample is in the magnetic field maximum, the total power dissipated in the sample is given by [12]

$$L = \frac{1}{2\sigma_1 \delta} \int_S |\mathbf{K}|^2 dS \tag{102}$$

with

$$\frac{1}{\sigma_1 \delta} = \frac{4\pi}{c_o} R_s. \tag{103}$$

The integral in Eq. (102) is over the surface of the spheroid and $\mathbf{K}$ is the effective surface current given by

$$\mathbf{K} = \int_0^\infty \mathbf{J} d\zeta = \frac{c_o}{4\pi} (\hat{e} \times \mathbf{H}), \tag{104}$$

where ζ is in the direction of the outward pointing normal vector to the surface $\hat{e}$ and $\mathbf{H}$ is the magnetic field at the surface of the spheroid. From Eq. (13) we can determine

$$\mathbf{H} = -\frac{\mathcal{H}_o}{n-1}. \tag{105}$$

The simplest way to solve this problem is to make use of prolate spheroidal coordinates [22]. In this coordinate system the three independent coordinates are given by u, v, and ϕ and the usual Cartesian coordinates are related to these through the transformation

$$x = d \sinh u \sin v \cos \phi \tag{106}$$

$$y = d \sinh u \sin v \sin \phi \tag{107}$$

$$z = d \cosh u \cos \phi, \tag{108}$$

where $d = \sqrt{a^2 - b^2}$ and a and b are the semi-major and semi-minor axes respectively. The three components of the metric are given by

$$h_u = d\sqrt{\cosh^2 u - \cos^2 v} \tag{109}$$

$$h_v = d\sqrt{\cosh^2 u - \cos^2 v} \tag{110}$$

$$h_\phi = d \sinh u \sin v. \tag{111}$$

The unit normal vector $\hat{e}$ is given by

$$\begin{aligned}\hat{e} = \hat{u} = \frac{1}{h_u}\frac{\partial \mathbf{r}}{\partial u} &= \frac{\cosh u \sin v \cos\phi}{\sqrt{\cosh^2 u - \cos^2 v}}\hat{x} \\ &+ \frac{\cosh u \sin v \sin\phi}{\sqrt{\cosh^2 u - \cos^2 v}}\hat{y} \\ &+ \frac{\sinh u \cos v}{\sqrt{\cosh^2 u - \cos^2 v}}\hat{z}. \end{aligned} \tag{112}$$

Assuming the external field is in the $\hat{z}$ direction leads to

$$|\mathbf{K}|^2 = \frac{c_o^2|\mathcal{H}_o|^2}{16\pi^2(n-1)^2}\left(\frac{\cosh^2 u \sin^2 v}{\cosh^2 u - \cos^2 v}\right). \tag{113}$$

Inserting Eq. (113) into Eq. (102) and using the fact that $dS = h_v h_\phi dv d\phi$ gives

$$L = \frac{c_o^2|\mathcal{H}_o|^2 \cosh^2 u_o \sinh u_o d^2}{32\pi^2\sigma_1\delta(n-1)^2}\int_0^{2\pi} d\phi \int_0^{\pi} dv \frac{\sin^3 v}{\sqrt{\cosh^2 u_o - \cos^2 v}}, \tag{114}$$

where $\cosh u_o = a/d$, $\sinh u_o = b/d$. From Eqs. (21) and (30) appropriate for the magnetic field, one finds

$$\mathrm{Im}\frac{\Delta\hat{\omega}}{\omega_o} = \frac{8\pi\gamma L}{|\mathcal{H}_o|^2 V_s \omega}. \tag{115}$$

The integral in Eq. (114) can be easily solved, and the resulting expression in Eq. (115) is proportional to the real part of the surface impedance. By analogy with Eq. (38) the resonator constant is given by

$$\begin{aligned}\xi &= \frac{-3ic_o\gamma d^2 \cosh^2 u_o \sinh u_o}{2b^2 a\omega(n-1)^2} \\ &\times \left\{\sinh u_o + (2 - \cosh^2 u_o)\arcsin\left|\frac{1}{\cosh u_o}\right|\right\}. \end{aligned} \tag{116}$$

References

[1] H. G. Beljers, *Physica* **14**, 629 (1949).

[2] J. G. Linhart, I. M. Templeton, and R. Dunsmuir, *Brit. J. Appl. Phys.* **7**, 36 (1956).

[3] L. D. Landau and E. M. Lifschitz, *Electrodynamics of Continuous Media* (Pergamon, Oxford, 1984).

[4] K. S. Champlin and R. R. Krongard, *IRE Trans. Microwave Theory Techn.* **MIT-9**, 545 (1961).

[5] M. E. Brodwin and M. K. Parsons, *J. Appl. Phys.* **36**, 494 (1965).

[6] L. I. Buranov and I. F. Shchegolev, *Instrum. & Exp. Tech.* **14**, 528 (1971).

[7] M. Cohen, S. K. Khanna, W. J. Gunning, A. F. Garito, and A. J. Heeger, *Solid State Commun.* **17**, 367 (1975).

[8] N. P. Ong, *J. Appl. Phys.* **48**, 2935 (1977).

[9] S. Donovan, O. Klein, M. Dressel, K. Holczer, and G. Grüner, *Int. J. Infrared and Millimeter Waves* **14** (1993) (subsequent article).

[10] M. Dressel, S. Donovan, O. Klein, and G. Grüner, *Int. J. Infrared and Millimeter Waves* **14** (1993) (sub-subsequent article).

[11] L. D. Landau and E. M. Lifschitz, *Statistical Physics* (Pergamon, Oxford, 1984).

[12] J. D. Jackson, *Classical Electrodynamics* (John Wiley & Sons, New York, 1975).

[13] R. I. Joseph and E. Schlömann, *J. Appl. Phys.* **36**, 1579 (1965).

[14] J. A. Osborn, *Phys. Rev.* **67**, 351 (1945).

[15] A. B. Pippard, *Proc. R. Soc. Lond. A* **A216**, 547 (1953).

[16] G. E. H. Reuter and E. H. Sondheimer, *Proc. R. Soc. Lond. A* **195**, 336 (1948).

[17] C. H. Papas, *J. Appl. Phys.* **25**, 1552 (1954).

[18] R. W. Morse and H. V. Bohm, *Phys. Rev.* **108**, 1094 (1957).

[19] J. J. Bowman, T. B. A. Senior, and P. L. E. Uslenghi, *Electromagnetic and Acoustic Scattering by Simple Shapes* (Hemisphere, New York, 1987).

[20] H. W. Helberg and B. Wartenberg, *Z. angew. Phys.* **20**, 505 (1966).

[21] F. Wooten, *Optical Properties of Solids* (Academic Press, San Diego, 1972).

[22] G. Arfken, *Mathematical Methods for Physicists* (Academic Press, New York, 1970).